

Extremely Nondegenerate Two-photon Processes in Semiconductors

David J. Hagan^{1,2}, Himansu S. Pattanaik¹, Peng Zhao¹, Matthew Reichert³
and Eric W. Van Stryland^{1,2}

¹CREOL, The College of Optics and Photonics, University of Central Florida, P.O. Box 162700,
Orlando, FL 32816-2700, U.S.A.

²Department of Physics, University of Central Florida, Orlando, FL 32816, U.S.A.

³Department of Electrical Engineering, Princeton University, Princeton, NJ 08455 U.S.A.

Keywords: Nonlinear Optics, Semiconductors, Infrared Detectors, Semiconductor Lasers.

Abstract: Direct-gap semiconductors show enhanced two-photon absorption and nonlinear refraction for the extremely non-degenerate case, i.e. for two light waves of very different wavelength, as compared to the degenerate case. We have verified this through measurements of non-degenerate two-photon absorption and nonlinear refraction in several direct-gap semiconductors. We have demonstrated application towards mid-infrared detection and imaging, as well as 2-photon gain in the mid infrared. We also show how semiconductor quantum wells may be employed to engineer even larger enhancements of these effects.

1 INTRODUCTION

Two-photon absorption (2PA) in direct-gap semiconductors has been extensively studied both experimentally and theoretically, resulting in the development of well-established scaling rules that predict the 2PA coefficient of direct-gap semiconductors. (Van Stryland, et al., 1985) The 2PA coefficient, α_2 is defined by,

$$\frac{dI}{dz} = -\alpha_2 I^2, \quad (1)$$

where I is the optical irradiance and z is the propagation depth inside the nonlinear material. α_2 is found to scale as E_g^{-3} , where E_g is the band-gap energy. Therefore, 2PA coefficients in narrow-gap semiconductors may be several orders of magnitude greater than in large-gap semiconductors. For example, in InSb where $E_g = 0.23$ eV, it is found that $\alpha_2 \approx 2$ cm/MW in the wavelength range 8 to 12 μm , while for ZnO, for which $E_g = 3.2$ eV, $\alpha_2 \approx 5$ cm/GW at a wavelength of 532 nm. This scaling law may be applied with similarly accurate predictions for any direct gap semiconductor.

Moving to the nondegenerate case, where two photons at different frequencies, ω_1 and ω_2 , with corresponding irradiances, I_1 and I_2 , are

simultaneously absorbed, the 2PA coefficient should be redefined as,

$$\frac{dI_1}{dz} = -2\alpha_2(\omega_1; \omega_2)I_2I_1 \quad (2)$$

where the order of the frequencies in the argument is important. Here it indicates that here we are observing the change in irradiance at ω_1 due to the presence of light at ω_2 . Nondegenerate 2PA was predicted (Sheik-Bahae, et al., 1991) to follow:

$$\alpha_2(\omega_1; \omega_2) = K \frac{\sqrt{E_p}}{n_1 n_2 E_g^3} F_2\left(\frac{\hbar\omega_1}{E_g}; \frac{\hbar\omega_2}{E_g}\right), \quad (3)$$

where,

$$F_2(x_1; x_2) = \frac{(x_1 + x_2 - 1)^{\frac{3}{2}}}{2^7 x_1 x_2^2} \left(\frac{1}{x_1} + \frac{1}{x_2}\right)^2 \quad (4)$$

where E_p is the Kane energy parameter, E_g is the bandgap energy, n_1 and n_2 the respective refraction indices and K is a parameter which is almost material-independent, usually taken to be $3100 \text{ cm GW}^{-1} \text{ eV}^{5/2}$ where all energies are in eV (Sheik-Bahae, et al., 1991). Note that this predicts 2PA to become very large in the extremely nondegenerate case, ($\omega_1 \gg \omega_2$). In 2011, our group experimentally demonstrated that these theoretical predictions work well for several direct-gap semiconductors. We have observed

nondegenerate 2PA coefficients as large as 1 cm/MW in CdTe, which is similar to the degenerate 2PA coefficient of InSb at 10.6 μm (Cirloganu, et al., 2011) Figure 1 summarizes these early results.

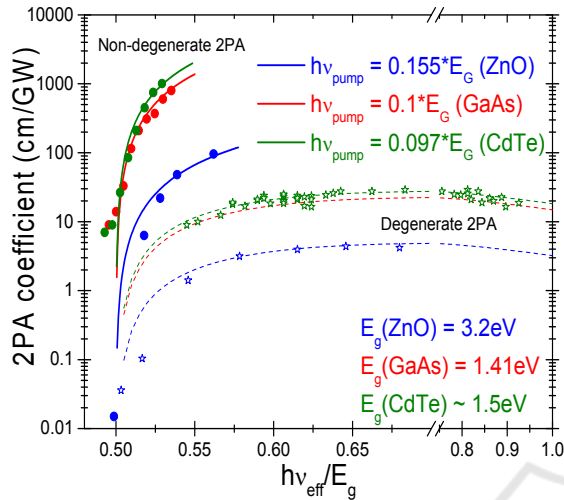


Figure 1: 2PA coefficient as a function of probe wavelength normalized by the bandgap energy for ZnO, GaAs, and CdTe. The solid lines are the prediction of the simple 2-parabolic band model. The dashed lines are for the degenerate 2PA along with associated data. (After Cirloganu, et al., 2011).

This strong enhancement opens up a number of possible applications for 2PA. As we shall describe in this paper, we have demonstrated highly sensitive gated infrared detection via 2PA using conventional semiconductor photodiodes. (Fishman, et al. 2011, Pattanaik, et al., 2016a) We have also investigated and demonstrated that 2-photon gain is similarly enhanced in the nondegenerate case, leading to the tantalizing possibility of 2-photon semiconductor laser devices. (Ironsides, 1992). Additionally, we have now shown that, as one might expect by causality, the enhancement in 2PA for the nondegenerate case translates directly to an enhancement of the bound-electronic nonlinear refraction (NLR) (Sheik-Bahae, et al., 1991). We describe our recent results that verify this strong nondegenerate NLR and its large anomalous dispersion above the 2PA edge. Finally, we show theoretically that the nondegenerate 2PA and consequently the 2-photon gain may be enhanced by yet another order of magnitude by employing quantum well geometries.

2 EXPERIMENTAL RESULTS

2.1 Infrared Detection using Nondegenerate 2PA

In 2011, we first demonstrated infrared detection with standard GaN and GaAs photodiodes using extremely nondegenerate photon pairs with up to 14:1 energy ratio (Fishman, et al. 2011). For detection in GaN, we used a 390 nm strong “gating” pulse, of 100 fs duration to sensitize a GaN pin photodiode to mid IR radiation. Mid IR pulses at 5.6 μm were detected when the gate and IR pulses were temporally coincident on the detector. The minimum detected IR pulse energy in uncooled GaN is as low as 20 pJ, while under identical conditions for a standard cooled MCT detector, the minimum detectable energy is 200 pJ. Although the quantum efficiency of such detectors is not quite as high as for a traditional interband detector, the noise is very low, due to the ultrafast gating. We have now also demonstrated cw detection using this method, although the sensitivity is not high in this case.

Since the detection requires temporal overlap between signal and gating pulses, it automatically provides information about the time of arrival of the signal pulse. We have recently applied this to 3-D infrared imaging of remote objects, as shown in Figure 2. (Pattanaik, et al., 2016a) It is worth noting that this process does not use IR crystals or phase-matching, as employed by upconversion detection which is based on second-order nonlinearities.

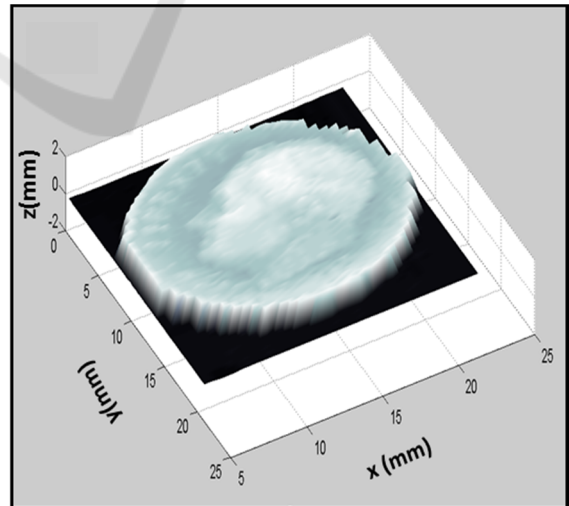


Figure 2: 2PA-detected 3-D image of a US 10-cent coin. (After Pattanaik, et al., 2016a).

2.2 Application to 2-Photon Gain

Based on reciprocity between absorption and gain, we also expect a similar effect for the reverse process of 2-photon gain (2PG). Taking the verified theory for 2PA to calculate the 2PG coefficient we find: (Ironsides, 1992)

$$\gamma_2(\omega_1; \omega_2) = K \frac{\sqrt{E_p}}{n_1 n_2 E_g^3} F_2\left(\frac{\hbar\omega_1}{E_g}; \frac{\hbar\omega_2}{E_g}\right) \times \{f_c(\hbar\omega_1; \hbar\omega_2) - f_v(\hbar\omega_1; \hbar\omega_2)\} \quad (5)$$

where γ_2 is the 2-photon gain coefficient which is positive in the case of a population inversion ($f_c > f_v$). The nondegenerate enhancement in this case may be applied to the generation of tunable mid-IR radiation. In Figure 3, we plot the gain as calculated by Equation 5 for cooled bulk GaAs with a population inversion. The gain coefficient is plotted versus the sum of the two photon energies as the larger photon energy is varied for several fixed values of the smaller photon energy. The degenerate 2PG coefficient is also shown for comparison.

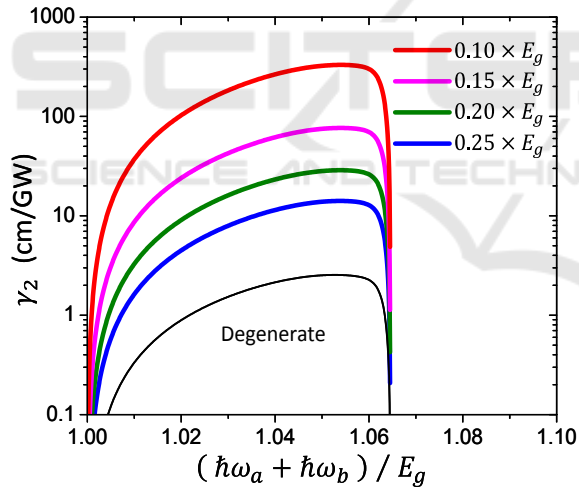


Figure 3: 2PG coefficient versus photon energy sum for bulk GaAs at 20 K with $N = 2 \times 10^{18} \text{ cm}^{-3}$ for several values of the nondegeneracy, e.g. $0.10E_g$ has IR photons of 0.15 eV or $\lambda = 8.2 \text{ }\mu\text{m}$.

We present experimental data showing extremely nondegenerate two-photon gain in bulk GaAs via pump-probe experiments with an additional optical excitation to generate a population inversion. A commercial Ti:sapphire chirped-pulse amplifier system producing 50 fs (FWHM) pulses at 800 nm and 1 kHz repetition rate is used as an excitation to generate population inversion in a 4 μm thick GaAs

sample. An optical parametric generator/amplifier with a difference frequency generator (AgGaS₂) is tuned to produce pulses of wavelength 7.75 μm in the mid-IR, and focused onto the GaAs to be used as a pump. A white-light continuum is filtered via narrow bandpass filters (10 nm FWHM) from 977 nm to 947 nm for use as a probe. The pump and probe photon energies add to be slightly greater than the bandgap energy of GaAs, where population inversion is obtained. Changes in transmission of the probe are monitored as the temporal delay between the pulses is varied. In the absence of above-gap excitation, the transmittance decreases as the pump and probe are overlapped in time, which one would expect for 2PA. This is indicated by the green squares in Figure 4. When the above-gap excitation at 800 nm is turned on so as to produce a population inversion, we expect both 2PG and free-carrier absorption (FCA). After using polarization discrimination to eliminate effects of FCA, as described in (Reichert, et al., 2016), we are able to observe nondegenerate two-photon gain, as shown by the blue circles in Figure 4. Although we observe 2PG, we note that the background losses due to FCA still surpass the gain, and the observation of net gain remains a challenge.

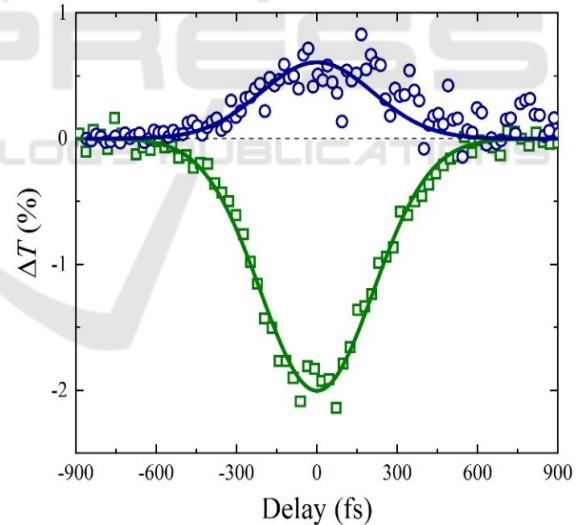


Figure 4: The transmittance change as a function of temporal delay between a 7.75 μm pump pulse and a 0.977 μm probe without (green squares) and with (blue circles) an above-gap excitation pulse that creates a population inversion in GaAs. (After Reichert, et al., 2016).

2.3 Nondegenerate Nonlinear Refraction

In addition to the extremely nondegenerate 2PA enhancement, our theory predicts that the nonlinear

refractive index $n_2(\omega_1; \omega_2)$ is also enhanced for very different frequencies. Precise knowledge of the magnitude, sign, and dispersion of n_2 is needed for design and prediction of Kerr-effect-based photonic devices such as all-optical switching. Our earlier theory relates the dispersion of n_2 to nonlinear absorption spectra via a Kramers-Kronig transformation, where the major contributing NLA mechanisms include 2PA, electronic Raman and the optical (AC) Stark effect. (Sheik-Bahae, et al., 1991) While the degenerate NLR coefficient $n_2(\omega; \omega)$ has been measured via the Z-scan method (Sheik-Bahae, et al., 1990), the nondegenerate NLR, namely the refractive index change at frequency ω_1 due to the presence of a beam at frequency ω_2 , of coefficient $n_2(\omega_1; \omega_2)$, is much less explored experimentally, particularly for the extremely nondegenerate case (i.e., $\hbar\omega_1 \gg \hbar\omega_2$) and for spectral regions where 2PA is present.

Here we describe the results of experiments that use a 2-beam method, nonlinear beam deflection, for the measurement of nondegenerate NLR (Ferdinandus, et al., 2013). Beam deflection utilizes a strong excitation pulse at ω_2 to create an index change at the sample that is sensed by the probe pulse at ω_1 . The index change deflects the probe by a small angle which is measured using a segmented detector by taking the difference of the energy falling on the left and right halves, $\Delta E = E_{left} - E_{right}$. By normalizing to the total energy E , $\Delta E/E$ is directly proportional to $n_2(\omega_1; \omega_2)$, and the transmission change for the E gives the NLA and hence the 2PA. We use a Ti:sapphire laser system to pump an optical parametric generator/amplifier to generate the excitation pulses from the idler beam at a wavelength of $\lambda_2 = 2.3 \mu\text{m}$. A portion of the 800 nm laser output is used to generate a white-light continuum (WLC) to be used as the probe. The NLR is measured at several wavelengths by filtering the WLC using narrow bandpass filters of bandwidth in the range 10-25 nm FWHM. The strong group-velocity mismatch between the pump and probe pulses has to be accounted for in determining the n_2 . We measured the dispersion of the nondegenerate NLR in the direct-gap semiconductors ZnO, ZnSe and CdS. In Figure 5, we show the measured nondegenerate n_2 for ZnSe. We see that the measured n_2 follows the theoretical prediction closely. However, we note that the nondegenerate enhancement in NLR is not as large as the enhancement of 2PA.

We are still looking for applications for the enhanced NLR. The difficulty is that the regions where it is enhanced are the same regions where 2PA is enhanced. We have also performed experiments at

wavelengths at the zero crossing for n_2 using femtosecond pulses. These pulses are spectrally broad, and we observe that different parts of the pulse undergo different signs of NLR as is predicted by our theory. This unusual behaviour may have some unique applications. For example, combined with anomalous dispersion, this effect could be applied to the reduction of chirp in optical pulses.

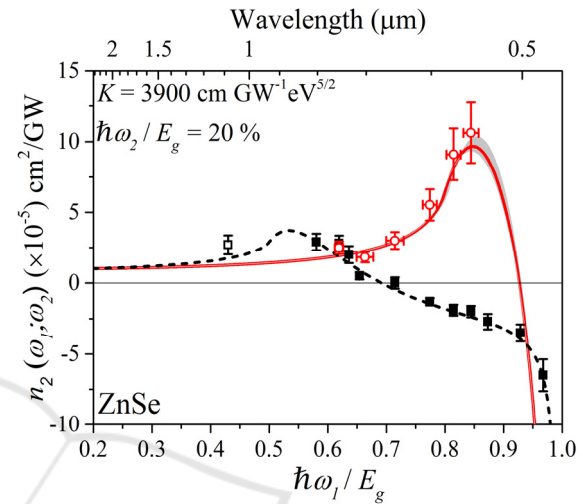


Figure 5: Measured $n_2(\omega_1; \omega_2)$ dispersion (red circles) of ZnSe, compared to theoretical calculations for nondegenerate (solid lines) and degenerate (dashed lines) n_2 ; Shaded region represents errors from the bandwidth of the excitation pulse; Degenerate n_2 data is shown for comparison (black squares).

2.4 Nondegenerate 2PA in Semiconductor Quantum Wells

Due to their large density of states near the band edge, it is expected that nondegenerate 2PA will be enhanced even more in quantum well (QW) structures than in the bulk. QWs show different linear and nonlinear optical properties when the incident light electric field vector polarized is changed from being in the plane of the QW (TE) to perpendicular to it (TM). We have developed a theory for ND-2PA in QWs using second-order perturbation theory and analytical expressions for the ND-2PA coefficient are derived for the different polarization combinations. (Pattaniak, et al., 2016b)

Our results indicate that TM-TM polarization gives the greatest enhancement, and we show results for this geometry. Figure 6 shows the 2PA coefficient calculated for different well thicknesses (each with infinite well depth) as a function of the normalized total photon energy. The normalization is done in such a way that the turn-on of linear absorption occurs at

the same energy, i.e., with respect to the one-photon transition energies. This allows comparison of the ND-2PA coefficient for the bulk and QW semiconductors on the same scale and also makes comparison to the respective degenerate 2PA coefficient easier.

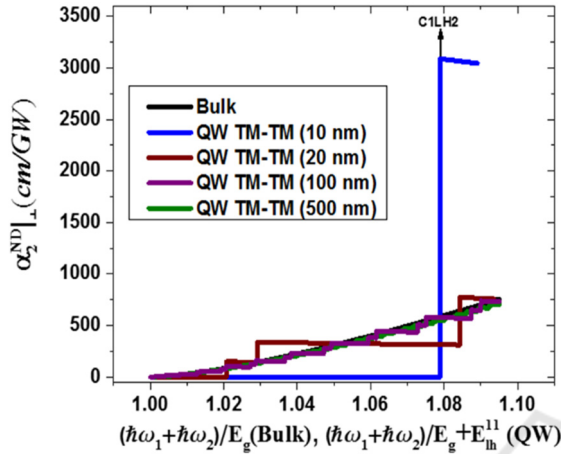


Figure 6: Nondegenerate 2PA coefficient in bulk GaAs and GaAs QW's of different widths for the TM-TM case. The arrows indicate valence band to conduction band transition energies.

Due to the large energy difference of photon pairs in the nondegenerate case, for a bulk semiconductor there is about a hundred-fold increase in $\alpha_2(\omega_1; \omega_2)$ over the degenerate case. The plot in Figure 6 is generated for a pump photon energy $\hbar\omega_2 \approx 0.12E_g$, corresponding to a wavelength of 7.5 μm and by varying the probe photon energy $\hbar\omega_1$. We have restricted the probe photon energy, $\hbar\omega_1$, to be at least 30 meV below the linear Urbach-tail absorption edge. This is done to keep the linear Urbach-tail absorption low. In a QW of width 10 nm, we obtain a maximum value for the nondegenerate 2PA coefficient of $\alpha_2(\omega_1; \omega_2) \approx 3000 \text{ cm/GW}$ which is approximately 36 times larger than predicted and measured in the bulk. These conditions of large enhancement correspond to where the mid-IR photon is near resonance with the inter-sub-band transition.

3 CONCLUSIONS

We have predicted and verified that the use of highly nondegenerate photon energies in two-photon processes in direct-gap semiconductors leads to strongly enhanced nonlinear effects. This in turn has led to the demonstration of sensitive mid-infrared detection and imaging using large bandgap

semiconductor detectors. It has also led to the observation of 2-photon gain in an optically pumped semiconductor. As expected via causality, 2-photon processes are accompanied by nonlinear refraction which is also measured to be enhanced in the extremely nondegenerate case. We have calculated that the effects of 2-photon absorption and 2-photon gain should be considerably larger in quantum wells than in bulk.

ACKNOWLEDGEMENTS

We thank Greg Salamo at the University of Arkansas for preparing the GaAs sample, and Arthur Smirl of the University of Iowa and Jacob Khurgin of Johns Hopkins University for stimulating discussions. This work was supported by the National Science Foundation Grants ECCS-1202471, ECCS-1229563, and DMR-1609895.

REFERENCES

- Cirloganu, C. M., Padilha, L.A., Fishman, D. A., Webster, S., Hagan, D. J., and Van Stryland, E. W., 2011, *Opt. Express* 19, 22951-22960.
- Ferdinandus, M. R., Hu, H., Reichert, M., Hagan, D. J., and Van Stryland, E. W., 2013, *Opt. Lett.* 38, 3518-3521.
- Fishman, D. A., Cirloganu, C. M., Webster, S., Padilha, L.A., Monroe, M., Hagan, D. J., and Van Stryland, E. W 2011, *Nature Photonics* 5, 561-565 (2011).
- Ironside, C. N., 1992, *IEEE J. Quantum Electron.*, 28, 842-847.
- Pattanaik, H.S., Reichert, M., Hagan, D.J., and Van Stryland, E. W., 2016a, *Opt. Express* 24, 1196-1205.
- Pattanaik, H.S., Reichert, M., Khurgin, J. B., Hagan, D.J., and Van Stryland, E. W., 2016b, *IEEE J. Quantum Electron.*, 52, 9000114-1--9000114-14.
- Reichert, M., Smirl, A.L., Salamo, G., Hagan, D. J., and Van Stryland, E. W., 2016, *Phys. Rev. Lett.* 117, 073602.
- Sheik-Bahae, M., Said, A.A., Wei, T.-H., Hagan, D.J., and Van Stryland, E.W., 1990, *J. Quant. Electron.*, 26, 760-769.
- Sheik-Bahae, M., Hutchings, D. C., Hagan, D. J. and Van Stryland, E. W., 1991, *IEEE J. Quant. Electron.* 27, 1296-1309.
- Van Stryland, E. W., Woodall, M.A., Vanherzeele, H, and Soileau, M. J., 1985, *Opt. Lett.* 10, 490.